J Mol Model (2004) 10:305–316
DOI 10.1007/s00894-004-0196-7

ORIGINAL PAPER

Mathias-Costa Blaise · Ramanathan Sowdhamini · Metpally Raghu Prasad Rao · Nithyananda Pradhan

Evolutionary trace analysis of ionotropic glutamate receptor sequences and modeling the interactions of agonists with different NMDA receptor subunits

Received: 23 January 2004 / Accepted: 3 June 2004 / Published online: 22 October 2004

Abstract The ionotropic *N*-methyl-D-aspartate (NMDA) receptor is of importance in neuronal development, functioning, and degeneration in the mammalian central nervous system. The functional NMDA receptor is a heterotetramer comprising two NR1 and two NR2 or NR3 subunits. We have carried out evolutionary trace (ET) analysis of forty ionotropic glutamate receptor (IGRs) sequences to identify and characterize the residues forming the binding socket. We have also modeled the ligand binding core (S1S2) of NMDA receptor subunits using the recently available crystal structure of NR1 subunit ligand binding core which shares ~40% homology with other NMDA receptor subunits. A short molecular dynamics simulation of the glycine-bound form of wild-type and double-mutated (D481N; K483Q) NR1 subunit structure shows considerable RMSD at the hinge region of S1S2 segment, where pore forming transmembrane helices are located in the native receptor. It is suggested that the disruption of domain closure could affect ion-channel activation and thereby lead to perturbations in normal animal behavior. In conclusion, we identified the amino acids that form the ligand-binding pocket in many ionotropic glutamate receptors and studied their hydrogen bonded and nonbonded interaction patterns. Finally, the disruption in the S1S2 domain conformation (of NR1 subunit- crystal structure) has been studied with a short molecular dynamics simulation and correlated with some experimental observations.

M.-C. Blaise · N. Pradhan (✉)
Department of Psychopharmacology,
National Institute of Mental Health
and Neuro Sciences (NIMHANS),
560029 Bangalore, India
e-mail: npr@nimhans.kar.nic.in
Tel.: +91 080 6995108
Fax: +91 080 6564830

R. Sowdhamini · M. R. P. Rao
National Centre for Biological Sciences (NCBS),
TIFR, UAS-GKVK Campus, 560065 Bangalore, India

Keywords NMDA · Ligand binding core · S1S2 segment · ET analysis · Homology modeling · Hydrogen bonding

Introduction

Glutamate receptor (GluR) channels play a major role in fast synaptic transmission. These receptors have been classified into three major subtypes, α-amino-3-hydroxy-5-methyl-4-isoxazole propionic acid (AMPA), kainate, and *N*-methyl-D-aspartate (NMDA) receptor channels. Of these, NMDA receptors have received very much attention because of their involvement in neuronal development, neurodegenerative diseases, and neuronal excitotoxicity. [1, 2] Voltage-dependent magnesium block and high calcium permeability of the NMDA receptors are of significance in certain types of learning and memory functions, namely, long-term potentiation. [3, 4] NMDA receptors are heterotetramers composed of two NMDA receptor subunit1 (NR1) and two of the four NMDA receptor subunit 2 (NR2A-2D) subunits. [5, 6] NMDA receptors are unique among the ligand-gated ion channels in their requirement for an obligatory co-agonist glycine in addition to the synaptically-released glutamate. [7, 8] Two independent glycine and glutamate binding sites located on the NR1 and NR2 subunits respectively, have been identified. [9a, 10] The role of the recently identified NR3 family of subunits (NR3A-3B) [11, 12] is yet to be visualized. At least two functional forms of NR3 have been identified: (a) the incorporation of NR3 subunit into NR1/NR2 receptor complexes resulting in NMDA receptors of reduced functionality [13, 14] (b) NR1/NR3 as an excitatory glycinergic receptor. [15]

The S1S2 ligand-binding core of the NR1 subunit of the NMDA receptor and the AMPA (Glr2) receptor has been crystallized [16, 17] with full and partial agonist-bound and antagonist-bound conformations. The S1 segment in the N-terminal and S2 segment in the linker between TM3-TM4 form the agonist-binding site. [18] The S1S2 structure reveals two lobes connected by a hinge

forming a clamshell-like structure similar to the bacterial periplasmic binding proteins. [19] As expected of domains serving common functions, the S1 and S2 segments are highly conserved. Different non-NMDA subunits have >50% amino acid identity whereas the NMDA and non-NMDA subunits have ~30% identity. [20] The glutamate receptor models reported here and a few of those recently published [21, 22] used the technique of fusing the S1 and S2 segments of AMPA, kainate and NMDA receptors with a hydrophilic linker to generate a water-soluble construct (S1S2) retaining the wild-type ligand binding affinity. [23, 24, 25]

An evolutionary trace (ET) analysis [26] was carried out on the S1S2 segment of 40 different ionotropic glutamate receptor sequences to identify the residues involved in forming the interface between S1 and S2 that may serve as targets for pharmaceutical design. The high-resolution crystal structure of NR1 [16] explains several of its family features, including agonist selectivity, activation, and desensitization. Here, we provide a structural rationale for agonist discrimination by NMDA receptor subunits [9b, 21, 22, 16] in terms of hydrogen bonding of amino acids forming the binding socket. All the subunits of the NMDA receptor share around 40% sequence identity with the crystal structure of NR1 (pdb code: 1pb7), while the kainate receptor (non-NMDA) shows higher sequence similarity (54% identity) with the known structure of the AMPA receptor (pdb code: 1ftj). Using this information, we modeled the NR2A, 2B, 3A and kainate receptor ligand-binding regions to explore the uniqueness of different ionotropic glutamate receptors (IGRs).

The essential role of the NR1 subunit in NMDA receptor functions has been confirmed in vivo by targeted disruptions of the NR1 gene. [27, 28, 29, 30] Homozygous mice with disrupted NR1 allele die of respiratory failure shortly after birth. [27] The targeted point mutations (*D481N*, *K483Q*) of the glycine binding site and the functional consequences of reduced glycine affinity of the NMDA receptor in mice have been studied extensively by several groups. [31, 32, 33] However, the molecular mechanism underlying this reduction in glycine affinity due to changes in S1S2 domain conformation after mutation remains elusive. To address this problem, we performed a short molecular dynamics simulation for 100 ps on both wild-type and double-mutated [*D481N*, *K483Q* (*NCBI protein database numbering*)] structures of the NR1 ligand binding core. Though the time duration is rather short to address the large conformational changes in the protein, it was enough to remove the constraints from the crystal structure and to observe the changes occurred at the hinge (linker) region in the S1S2 segment. The conformational changes observed in the S1S2 segment can be correlated with the reduction in glycine affinity and thereby with the behavioral abnormalities. [31, 32]

Materials and methods

The glutamate receptor primary sequences were obtained from the NCBI (protein) database and were analyzed using the BLAST [34] program. The information about the protein sequences used for the study is given in the Electronic Supplementary Material (ESM.1) Secondary structure prediction was carried out by PHDsec, [35] and CLUSTALX [36] was used for multiple sequence alignment. Receptors complexed with glycine (1pb7) and glutamate (1ftj) were used as templates for homology modeling of the NMDA and kainate receptor ligand binding sites, respectively. Twenty different models were prepared for each subunit of NMDA and non-NMDA ionotropic glutamate receptors using MODELLER. [37] The model with the lowest energy was considered as the ideal model. Verify3D [38] was used to check the 3D profile of the models while PROCHECK [39] was used to analyze the stereochemical properties. The evolutionary trace (ET) method (TraceSuite II) was used to determine the residues involved in ligand binding in different subtypes of glutamate receptors. The dendrogram obtained from the ET analysis was used to locate the evolutionary cut-off between the different IGRs. The models were subjected to energy minimization using the AMBER force field as available in the INSIGHTII molecular modeling software. [40] Hydrogen atoms were added to the protein models to facilitate the incorporation of hydrogen bonds. The N and C terminals of models were not charged during minimization. Molecular dynamics simulation was carried out at 300 k using the Discover3 program available in the INSIGHTII software to study the conformation of S1S2 segment.

Knowledge about the ligand-binding region of X-ray crystal structure of the NR1 and AMPA receptors was directly extrapolated to the other NMDA-receptor models and the mutagenesis data of the NMDA receptor [9a] were taken into account to determine the putative ligand-binding pocket. Each ligand was placed at the binding region and the ligand-receptor complex was optimized. An automated docking method in INSIGHTII was followed to dock the ligands. After docking, it automatically performed a short molecular dynamic simulation followed by docking to rearrange the conformation of the ligand–receptor complex at the minimum energy level. LSQMAN [41] was used to superimpose the models onto the template and evaluate the structural differences in the models. The amino-acid numbering used in Fig. 1 is followed throughout the article unless otherwise explicitly mentioned. The amino-acid number is mentioned in superscript when the NCBI protein database numbering is used. All the figures were prepared using the SPDBV molecular viewer program [42] and RASMOL. [43]

Results and discussion

Sequence analysis and multiple sequence alignment

Forty ionotropic glutamate receptor sequences were aligned with the AMPA and NR1 subunits (of the NMDA receptor) ligand binding core. Equivalent residues at the alignment position corresponding to the ligand-binding core were identified to get the S1S2 segment of all the IGRs. Derived multiple sequence alignment (see ESM.1) was used for the ET method and was further extended to model the NR2A, NR2B, NR3A, and kainate receptor ligand binding regions. The segment marked as S1 in Fig. 2 comprises mainly extended strands, while the S2 segment comprises strongly conserved helices including an amphipathic helix (5th α-helix in Fig. 2). Almost all the predicted secondary structures of the NMDA-receptor sequences align well with the observed secondary structures of AMPA and NR1. A 30-residue insertion at the S1

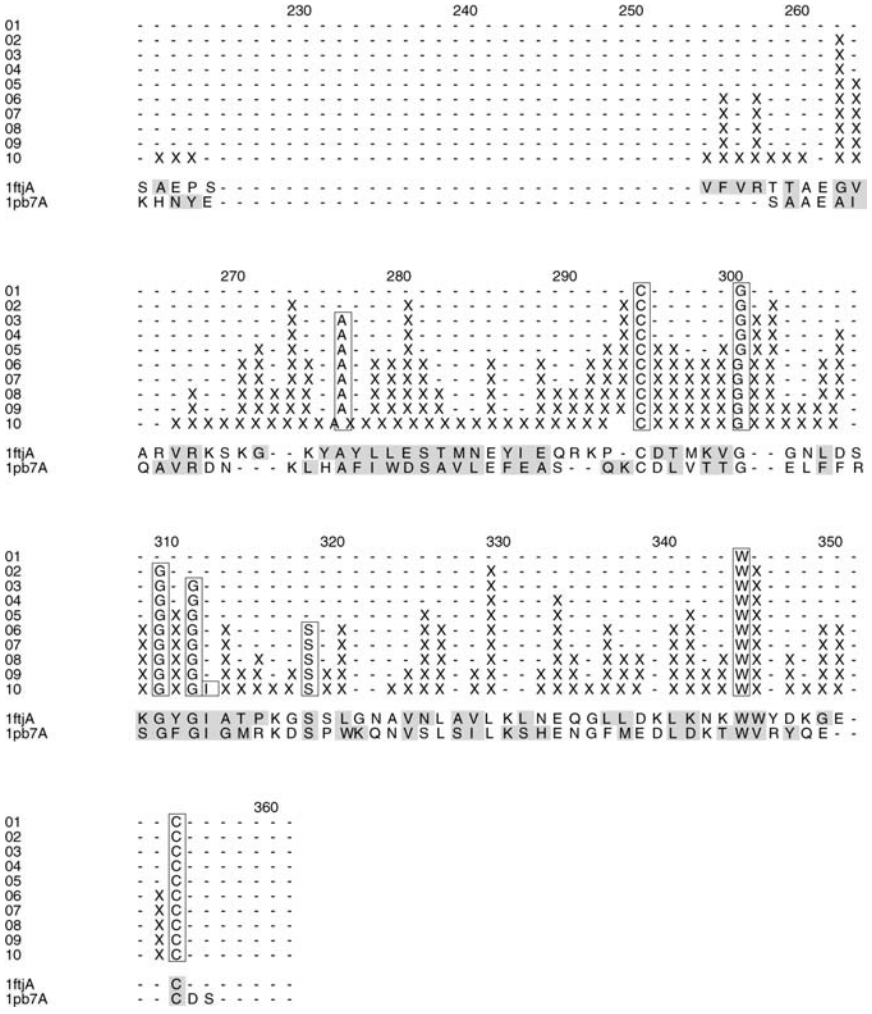

Fig. 1 Traces for partitions P01–P10 aligned with the amino acid sequence of glutamate receptor-2 (1ftj) and NR1 (1pb7) ligand binding core are shown. Conserved residues are given in *boxes*; class specific residues denoted by "X", and solvent accessible side chains are *shaded*. The amino acid numbering followed here is used throughout the analysis

segment is unique to the NMDA subtype of IGR, though the number of residues at the insertion varies with the subunits. Other IGRs such as AMPA or kainate do not include this insertion except for the *apteronotus leptorhynchus* AMPA receptor. In addition, NR1 consists of an "NKKE" insertion in S1, which may account for its peculiar physiological properties. The NR2 subunit of the NMDA receptors consists of several subtype-specific 2–4-residue insertions along the S2 segment, whereas the non-NMDA IGRs possess a group-specific four-residue insertion between the three highly conserved regions (see ESM.1). The glutamate receptor (*Glr7*) of *Caenorhabditis elegans* has a 30-residue insertion after the *227th* residue in the alignment whereas the *Glr1* of *C. elegans* consists of 15-residue insertions.

Evolutionary trace (ET) analysis

As opposed to drastic changes such as insertions and deletions, several amino acid exchanges at equivalent positions often impart specific substrate recognition and functional differences to homologous sequences. ET analysis provides a quantitative insight into the relationship between all the IGRs by locating the exchanges at ten different partitions (Fig. 3) according to their common evolutionary time cut-off (ETC). ET analysis is guided by two observations: First, protein structures descending from a common ancestor are remarkably similar, with backbone deviations remaining within 2 Å even when the sequence identity falls to 25%. [44] Second, the active site residues under evolutionary pressure tend to maintain their functional integrity and undergo fewer mutations than functionally less important amino acids. [45] These observations imply that evolutionarily related sequences can be compared with each other to extract the structural and functional data. [46, 47]

The crystal structures of AMPA and NR1 indicate the involvement of α-helices 1 and 3 of the S1 segment in the intersubunit interaction in all the IGRs (Fig. 2). The loop between helices 5 and 6 may contribute to the formation of oligomers in the AMPA-glutamate receptor. Sixteen residues are found to be invariant at the ligand binding region of the IGR family. However, a number of residues are identified as class-specific and may play a role in subtype-specific activity in the IGRs (Fig. 1). All the invariant residues are tabulated (Table 1) to depict their locations and structural and functional importance.

Fig. 1 (continued)

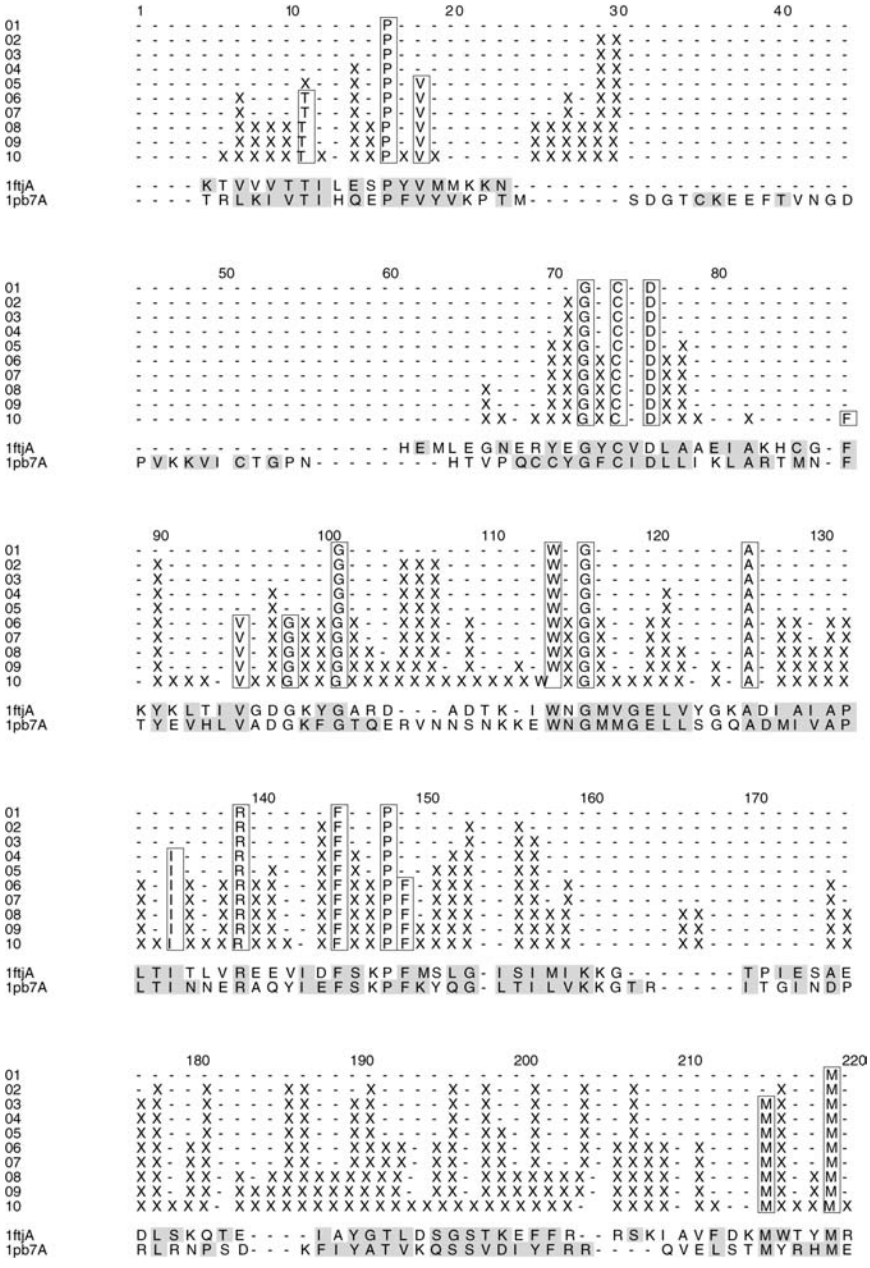

Among all the invariant residues, *Arg139* and *Phe145* are directly involved in ligand binding and intersubunit interaction, respectively, while other residues contribute to form the skeleton of the IGRs. The interaction of *Phe145* with the antiparallel β-sheet formed by the 5th and 9th β-strands may be structurally important.

A residue important in determining the affinity or the specificity of an interaction inside a given subgroup may only play a minor role in a similar event for other groups of molecules. For instant, $Lys^{483}99$ in the NR1 subunit of the NMDA receptor is crucial for channel activation [31, 32] whereas its loss in kainate (KA2) receptors does not affect the equivalent process. Invariably, a bulky aromatic group is needed at the 100th position to form the binding pocket in all IGRs. An invariant cysteine residue, *Cys355* located next to the 10th α-helix is involved in disulfide bond formation with another invariant *Cys295* residue located in front of the 7th α-helix (Fig. 2). This cross-link is of importance in producing a natural restraint on domain movement during ligand binding. A detailed diagram about the location of conserved and class-specific residues is given in Fig. 4. A class-specific residue (*Asp71*) located after the second β-strand is expected to be involved in oligomerization. On the other hand, the NMDA subtype of glutamate receptors contains a 30-residue insertion at this region, which may be responsible for intersubunit interaction.

Residues involved in ligand–receptor interaction are tabulated (Table 2) and their characters have been studied. A conserved glutamic acid (*Glu14*, present in between b1 and b2) is replaced by glutamine in the NR1 subunit of the NMDA receptor, which is physiologically and phar-

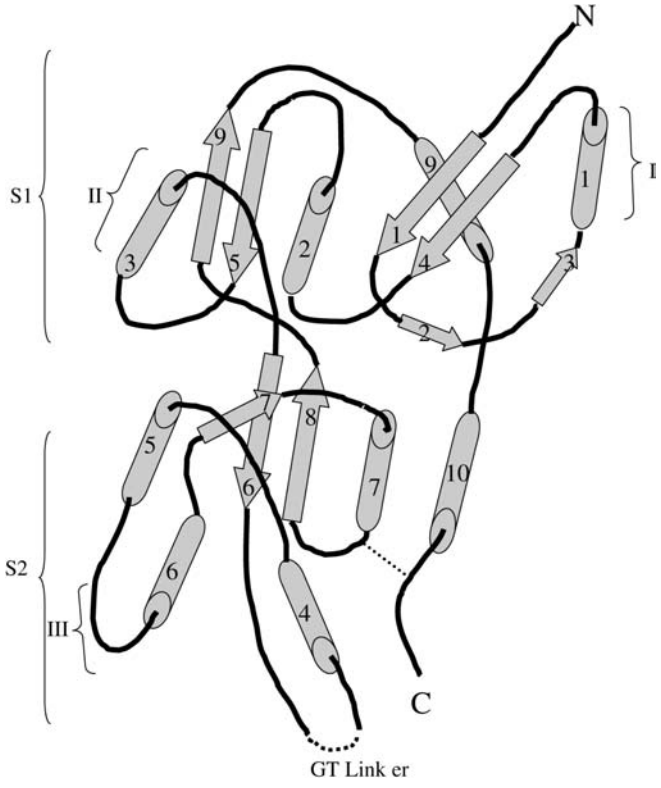

Fig. 2 Topology diagram of the ligand-binding core of IGRs: α-helix and β-strand positions are numbered and represented by *cylinders* and *arrowhead* ribbons, respectively. I, II and III are regions involved in tetramerization in all the IGRs. The two segments S1 S2 are closed upon ligand binding and these are joined together by Gly–Thr (GT) linker. The disulphide (S–S) bond after the 7th and 10th α-helix is a characteristic conserved feature for IGRs

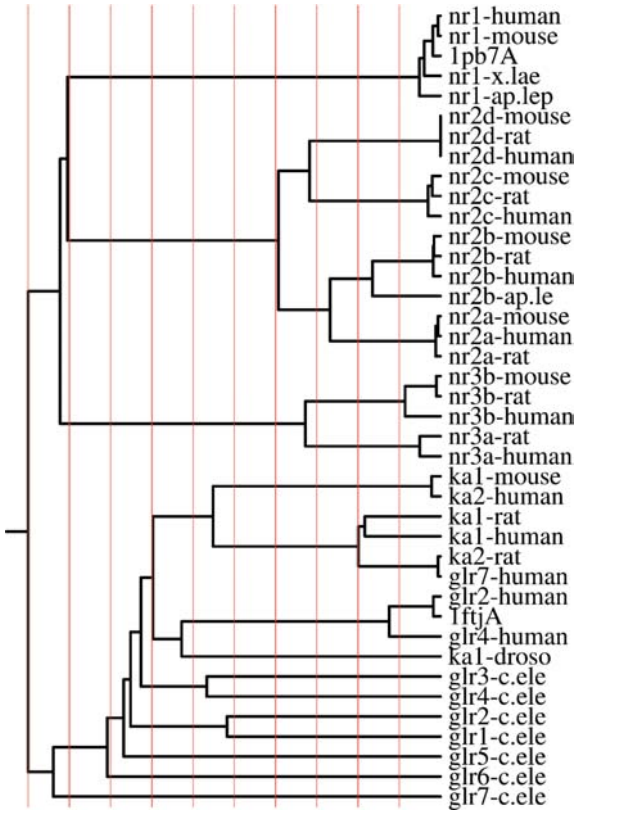

Fig. 3 Sequence dissimilarity-based dendrogram for ionotropic glutamate receptor ligand binding core sequences are shown. The vertical lines show the partitions considered for evolutionary analysis

Table 1 The location, structure, and functional importance of all invariant residues forming ligand binding core identified by ET analysis

Sl. No	Invariant residue	Location	Structure/functional importance
1	*Pro16*	2nd β-strand	Backbone of 1st ligand binding motif
2	*Gly72*	1st α-helix	Forming the structurally conserved α-helix after a long non-conserved region
3	*Cys74*	1st α-helix	
4	*Asp76*	1st α-helix	
5	*Gly101*	Loop b/w 4th β and 2nd	Directly involved in ligand binding and projecting neighbor residues into the binding socket
6	*Trp114*	2st α-helix	Highly conserved α-helix but neither involved in ligand binding nor dimerisation
7	*Gly116*	2st α-helix	
8	*Ala126*	5th β-strand	Involved in forming an antiparallel β-sheet with 9th β-strand, which stabilizes the S1 domain
9	*Arg139*	3rd α-helix	To form a highly conserved α-helix which directly involved in both ligand binding and dimerisation
10	*Phe145*	3rd α-helix	
11	*Pro148*	3rd α-helix	
12	*Met219*	5th α-helix	Key role in forming an amphipathic helix which contains structural importance
13	*Cys295*	Loop b/w 7th α and 8th β	Making disulphide bond with Cys355 that creates restraint for domain movement
14	*Gly301*	8th β-strand	Involved in forming an antiparallel β-sheet with 5th β-strand, which stabilizes the S1 domain
15	*Trp345*	10th α-helix	Forming the structurally conserved α-helix
16	*Cys355*	Loop after 10th α-helix	Making disulphide bond with Cys295 that plays major role in domain movement

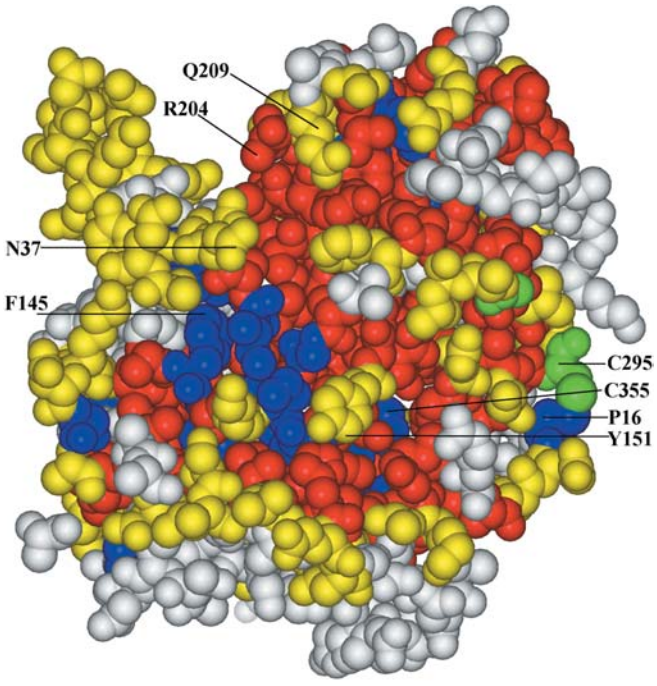

Fig. 4 The residues of partition P10 are mapped onto the known structure of NMDAR1 (1pb7). The color codings are as follows: conserved buried—*blue*; conserved exposed—*green*; class specific buried—*red*; and class-specific exposed—*yellow*. The structurally functionally important residues *Cys295* and *Cys355* form a disulphide bond between the S1 and S2 domain. *Phe145*, *Pro16*, *Gln209* and *Arg204* are involved in ligand binding while *Asn137* and *Tyr151* are involved in interactions with other subunits

macologically different from other glutamate receptors. Both residues at alignment positions *132* and *134* are believed to be involved in ligand binding. [16] AMPA and kainate receptors contain *Pro* and *Ala* residues at these two positions, respectively. However, the NMDA receptor, except in the NR1 subunit, has a class-specific *Ser* equivalent to this position. Residues present at the S2 segment of the ligand-binding core as well as in the S1 segment are important for the domain-closing mechanism. The highly conserved *Thr198* residue with its class-specific neighbor *Ser197* is believed to be involved in hydrogen bonded interactions with the ligand (detailed in the homology modeling and docking section). [1] NR3A subunits of NMDA receptors are reported to have different pharmacological activities to all other NMDA receptor subunits [14, 15] and contain a class-specific mutation at *136* (*Thr* to *Ser*) and *198* (*Thr* to *Ala*) position. Further, the NMDA receptor contains a common class-specific *Asp* residue at the *281* position which is crucial for domain closure, whereas AMPA and Kainate receptors contain a *Glu* residue at this position.

Homology modeling and docking

A three-dimensional model of NR2A, 2B, 3A and kainate receptor ligand-binding regions is obtained by homology modeling. The interactions of NR2A, 2B, 3A, and kainate receptors with their endogenous agonists are modeled and shown in Fig. 5a–d. The stereochemical properties of all the models are given in Table 3. Molecular dynamics studies [48, 49] reveal that each subunit of the glutamate receptor has a distinct domain-closing mechanism upon ligand binding, even though these subunits have a com-

Table 2 Residues involved in forming the ligand-binding pocket of different ionotropic glutamate receptors (NCBI database sequence numbering)

Sl.No	ET number	AMPA	Kainate	NR1	NR2A	NR2B	NR2C	NR2D	NR3A	NR3B
1	*14*	*E423*	*E424*	*Q393**	*E413*	*E413*	*E413*	*E439*	*E522*	*E424*
2	*99*	*K470*	*L471**	*K483*	*K484*	*K485*	*K482*	*K512*	*K604*	*K504*
3	100	Y471	Y472	F484	H485	H486	H483	H513	Y605	Y505
4	132	P499	A499	P516	S511	S512	S509	S539	S631	S531
5	**134**	**T501**	**T501**	**T518**	**T513**	**T514**	**T511**	**T541**	**S633****	**S533****
6	***139***	***R506***	***R506***	***R523***	***R518***	***R519***	***R516***	***R546***	***R638***	***R538***
7	***234***	***S675***	***S673***	***S688***	***S689***	***S690***	***S687***	***S717***	***S801***	***S701***
8	235	T676	T674	V689	T690	T691	T688	T718	A802	A702
9	**318**	**E726****	**E722****	**D732**	**D731**	**D732**	**D729**	**D759**	**D870**	**D745**

The 2nd column denotes the numbering used in evolutionary trace analysis (Fig. 1)
Bold denotes the invariant residues, italic is used to highlight the row where only one residue is different from all the others, which is marked by *. Bold italic is used to highlight the row where two residues are different from all the others, which are marked by **
Accession numbers for all the (human) glutamate receptor subunit sequences are given in ESM 2

Table 3 Summarized results of homology modeling

Query sequence	Template chosen (pdb code)	% Sequence identity (Q-T)	% Allowed region in Ramachandran plot
NR2A	1pb7	34	89.4
NR2B	1pb7	34	88.1
NR3A	1pb7	35	85.2
Kainate	1ftj	54	86.9

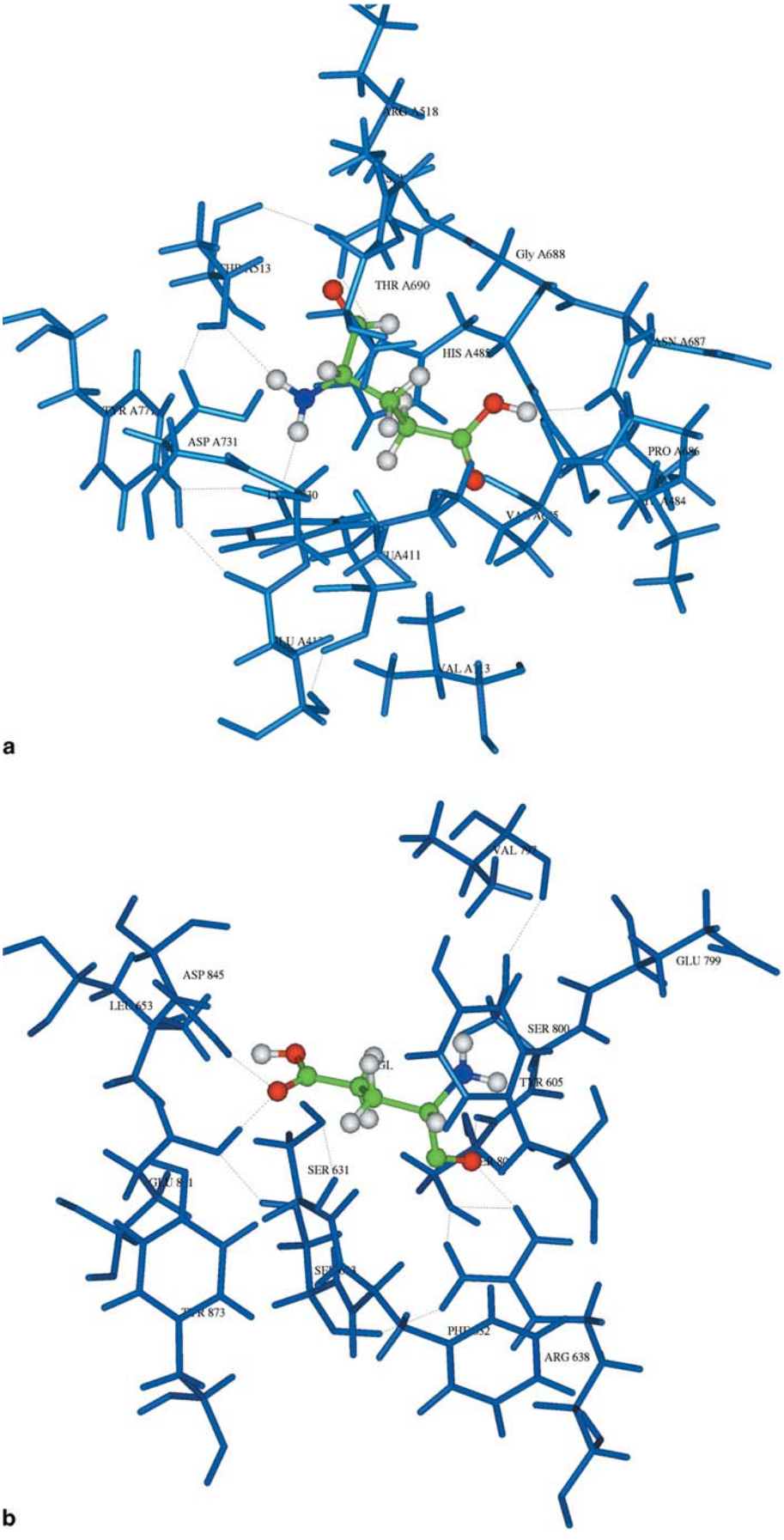

Fig. 5 a, b The binding mechanism of glutamate in the NR2A and NR2B subunits of the NMDA receptor, respectively. Glutamate is shown in *cpk*, hydrogen bonds in *dotted lines*, and amino acids in *blue*. The amino acids shown here are within 4 Å radius of the ligand (glutamate). Hydrogen bonds shown here are between the ligand and the receptor and also within the amino acids of 4-Å sphere. In the NR2A subunit, glutamate fails to make any interaction with *Arg139* (in **a**, it is *Arg518*) whereas in all other glutamate receptors it makes a salt bridge with *Arg139* (NCBI database numbering is followed to label the amino acids). **c, d** The binding mechanism of glutamate in NR3A and kainate receptors, respectively. Glutamate is shown in *cpk*, hydrogen bonds in *dotted lines*, and amino acids in *blue*. The amino acids shown here are within 4-Å radius of the ligand (glutamate). Hydrogen bonds shown here are between the ligand and receptor and also within the amino acids of 4-Å sphere (NCBI database numbering is followed to label the amino acids)

Fig. 5 (continued)

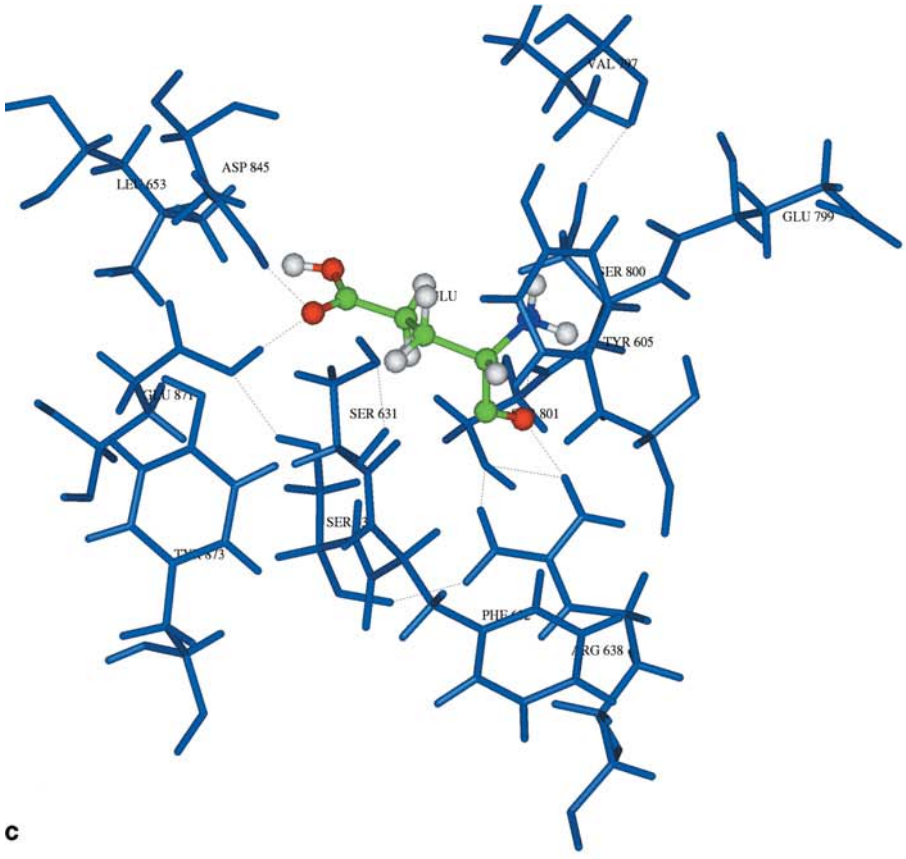

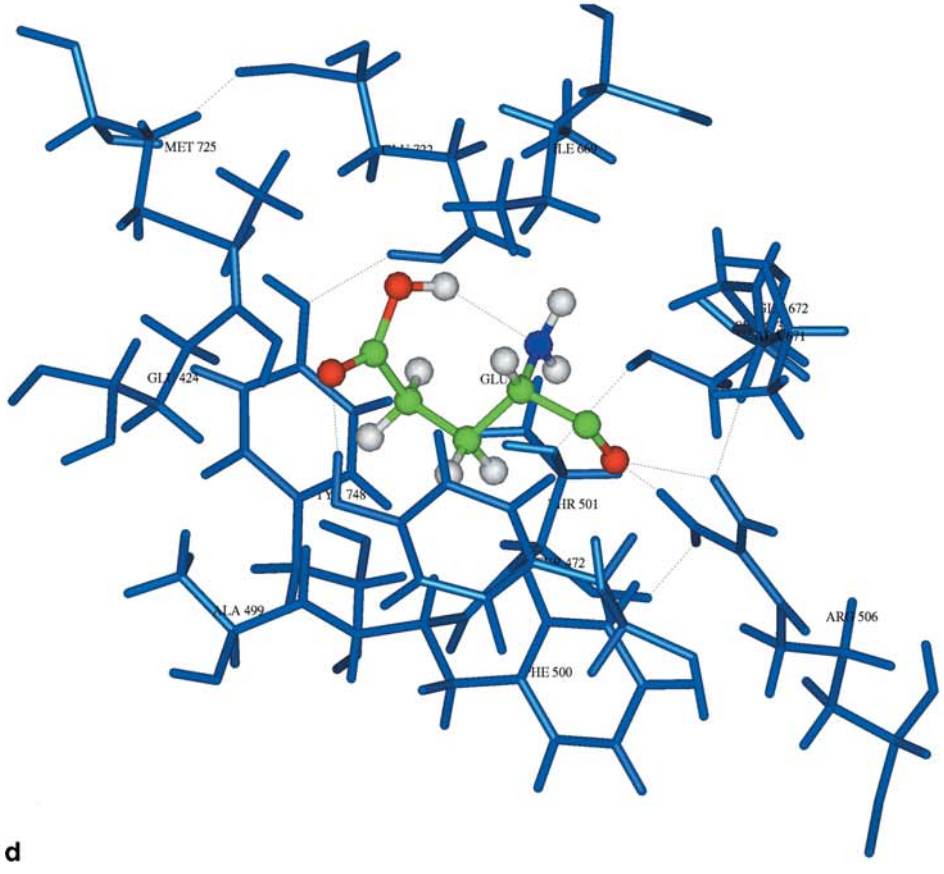

Table 4 Agonist–receptor (bonded) interacting pattern for glutamate receptors with their natural agonist glutamate and/or glycine

Sl.No	Subunit	Donor	Acceptor	Distance	Angle
1	NR1 (glycine)	R523: HH12	GLY:1:O	2.46	124.79
2		R523: HH21	GLY:1:O	1.97	144.39
3		T518:HN	GLY:2:O	2.39	123.41
4		R523: HH12	GLY:2:O	2.24	165.59
5		**GLY:2:HO**	P516:O	1.79	143.35
1	NRI $^{(D481N/K483Q)}$ (glycine)	R523: HH11	GLY:1:O	2.06	156.50
2		R523: HH21	GLY:1:O	2.13	143.90
3		**GLY:2:O**	P526:O	2.12	161.26
1	NR2A (glutamate)	T513:HG1	GLU:1:O	1.96	126.30
2		S639:HN	GLU:2:O	1.86	159.23
1	NR2B (glutamate)	H486:ND1	GLU:2:O	2.70	NA
2		R519:HH21	GLU:2:O	2.04	142.19
3		S690:HN	GLU:2:O	2.21	143.90
4		**GLU:2:O**	H486:ND1	1.80	159.19
1	NR3A (glutamate)	R638: HH11	GLU:1:O	2.06	142.98
2		S801:HN	GLU:1:O	2.25	133.17
3		D845:HD2	GLU:2:OE1	1.94	159.60
4		E870:HE2	GLU:2:OE1	2.00	160.34
5		GLY:2:HO	S631:O	1.84	148.42
1	Kainate (glutamate)	R506: HH11	GLU:1:O	1.82	134.66
2		R506: HH22	GLU:1:O	2.26	127.58
3		T501:HN	GLU:2:O	2.01	127.48
4		**GLU:2:HO**	T501:O	2.08	133.70

Bold is used to highlight the oxygen atom of either main chain (α-carboxyl group) or sidechain of the agonist acting as an electron donor in all the glutamate receptors except the NR2A subunit of NMDA receptor

The atom numberings in column 3 and column 4 are according to the INSIGHTII software (NA—not applicable)

mon architecture for their binding sockets. The carboxyl group of glutamic acid, the ligand, is involved in a salt-bridge with the guanidium group of *Arg139*. Invariably, all the glutamate receptors modeled here exhibit this feature except the NR2A subunit of the NMDA receptor. *Arg139* is located in the middle of the 3rd helix (Fig. 2) and the side chain projects towards the binding socket. The region after this α-helix is a short unstructured loop in several glutamate receptors including the AMPA receptor, whereas the NR1, 2A and 2B of the NMDA receptors contain a short helix between the 3rd helix and the 6th β-strand. Secondary structure prediction results confirm the presence of this helix in the NR1 subunit. We propose that this short helix may form (intersubunit) tertiary interactions in NMDA receptors. In addition to *Arg139*, the *132nd* (*Ser*-at NR3A and *Pro* at AMAPA, NR1) or *134th* (*Thr*- at NR1, 2A, 2B, AMPA, Kainate and *Ser* at NR3A) residues serve as electron acceptors, forming a hydrogen bond with the free oxygen atom of the glutamic acid side chain (Table 4). These results are in agreement with the existing information about glutamate–receptor ligand binding. [16] A positively charged residue *Lys99* located in the S1 segment is conserved in all glutamate receptors except kainate receptors, where it is replaced by a simple hydrophobic side chain residue *Leu*.

The residues present in the S2 segment near the interface between S1S2 are involved in S1S2 domain movements by forming bonded and non-bonded interactions with the agonist. For instance, the presence of class-specific residues at *197 and 198* suggests that the S1–S2 segments in NR2A and 2B are stabilized by hydrogen bonds (*Ser* and *Thr* respectively), whereas such an interaction is unlikely in NR1 and NR3A due to the substitution of *198* by *Val* and *Ala*, respectively. As compared with other glutamate receptors, the S2 segment of the NR1 subunit has a stronger interaction with the ligand by forming several H-bonded and non-bonded interactions. [16] The NR1 subunit shows a relatively larger *rmsd* between the open (antagonist) and closed (agonist) form than the other IGR subunits. [1] Our modeling and docking studies show that NR2A forms two-bonded interaction with the agonist (Fig. 5a), thereby closing the S1S2 domain. On the other hand, the kainate receptor S1S2 segment is tightly attached though its agonist (glutamate) does not make any hydrogen-bonded interactions with S2 segment, but it retains the highest number of non-bonded interactions with the S2 segment residues (Fig. 5d) among all the glutamate receptors examined here. The 1st or 2nd oxygen atom of the α-carboxyl group of glycine and glutamate acts as an electron acceptor to form a hydrogen bond with the electron-donating groups present at the guanidium group of the *Arg139* residue. The 2nd oxygen atom of the agonists (both glycine and glutamate) acts as an electron donor to make an H-bond with the residue present at the 132nd or 134th position of the glutamate receptor, but this kind of interaction is absent in the NR2A subunit of the NMDA receptor. Finally, the domain closure upon agonist binding depends on the exact location of the interacting residues in the S1 and S2 segments.

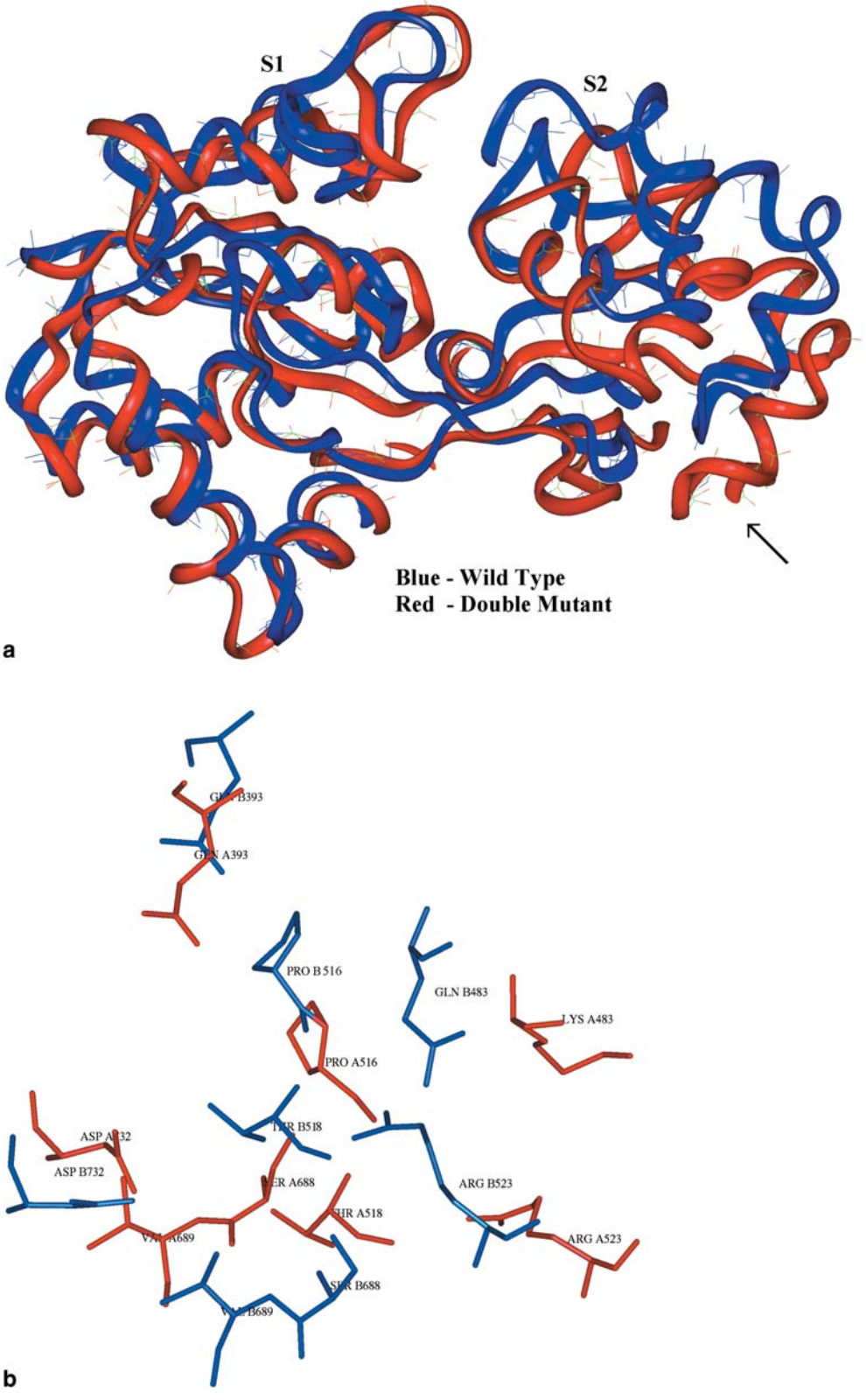

Fig. 6 a Wild type and double-mutated structures are superimposed by using LSQMAN. It indicates that the S2 domain is considerably detached from S1 when compared with the wild type after 100 ps of molecular dynamics simulation. The *arrow* denotes transmembrane helices (pore forming) region in the native IGRs. **b** Residues involved in ligand binding at both NR1-GRIN1$^{D481N/K483Q}$ structures are superimposed to calculate the rmsd (*blue*—wild type; *red*—double mutated). Ca atoms of these residues show ~3.5 Å rmsd between the wild-type and mutated structures. (NCBI database numbering is followed to label the amino acids)

Analysis of NR1$^{(D481N/K483Q)}$ mice ligand binding core

We have performed a comparative analysis of wild-type and doubly mutated (NR1$^{D481N/K483Q}$) NR1 starting from the available crystal structure of the wild type. Both *rmsd* and hydrogen bonding patterns in the glycine-bound form were compared to understand the impairment of NMDA receptor function in mice with these targeted point double mutations at the glycine-binding site. The glycine-bound form of the wild-type and double-mutant NR1 subunit

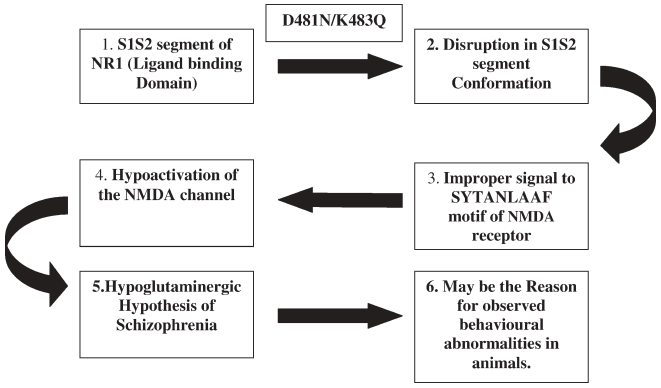

Fig. 7 Flow chart showing the step-by-step consequence of double mutation at NR1 ligand binding core that leads to behavioral abnormalities in experimental animals

structures were analyzed after 100 ps of molecular dynamics simulations. The doubly mutated structure shows ~2.0 Å rmsd with the wild type (Fig. 6a). The arrow mark at Fig. 6a points out the region where the S1S2 segments are joined by a GT (Gly–Thr) linker that constitutes the transmembrane (pore-forming) regions in the native IGRs. After simulation, the S1S2 hinge conformation was considerably changed between the wild type and the double mutant structures.

Not only the side-chain guanidium group of *Arg139* is pushed into the ligand binding shell by 2.0 Å, but also the binding-socket framework is completely collapsed and there are large changes (~3.5 Å rmsd) in the conformation of all the residues responsible for agonist binding (Fig. 6b). These differences may account for hypoactivation of the channel in the doubly mutated type. Fig. 7 shows the step-by-step consequences of double mutation at NR1 ligand binding core that lead to behavioral abnormalities in experimental animals. A drastic change was observed in agonist–receptor interacting pattern (Table 4) between wild and mutated structures as the latter failed to interact with $Thr134^{(T518)}$ and lost a favorable interaction with a free hydrogen atom at $Arg139^{(R523)}$. These findings can be directly correlated with existing knowledge about the importance of the NR1 subunit activation in animal behaviors (as shown in Fig. 7) and drug action. [31, 32, 33]

Conclusion

The present study was carried out for two reasons: firstly, for evolutionary trace analysis and homology modeling of different IGRs ligand binding cores; secondly, to study conformational analysis of the S1S2 segment (of the NR1 crystal structure) after a double mutation by molecular dynamics. These results together here provide information at the molecular level about the IGR S1S2 segment along with the importance of its conformation (at the hinge region) in channel activation by using the available NR1 crystal structure.

In the first part, ET analysis was used to identify the conservation patterns of each group to examine their similarities and to identify structurally and functionally important residues. Determining these residues is useful in explaining the functional discrepancies among the receptor types despite high sequence similarity of the ligand-binding core. G*lu* at the 14th position is functionally important in all the glutamate receptors as its α-acidic moiety is involved in a non-bonded interaction with the ligand (glutamate). Unlike all the other ionotropic receptors, the NR1 subunit contains *Gln* at this position, which could play a role for reduction in glutamate affinity.

In the second part, molecular dynamics simulations reveal that the S2 segment of a doubly mutated structure is considerably detached from the S1 segment, whereas it is fully closed in wild type. The detachment of S1S2 segments of the NR1 subunit in the doubly mutated form account for the change in the physiological and pharmacological properties of $NR1^{D481N/K483Q}$ mutated mice as the domain closure is inversely proportional to ion-channel activation.

Supplementary Material

The detailed sequence alignments and the table containing organism name, database and accession code are available as electronic supplementary materials ESM1 and ESM2, respectively in (http://link.spinger.de) .

Acknowledgements We thank Dr. Chittaranjan Andrade and Dr. Innis Axel for language correction of the manuscript.

References

1. Dingledine R, Borges K, Bowie D, Traynelis SF (1999) Pharmacol Rev 51:7–61
2. Cull-Candy S, Brickley S, Farrant M (2001) Curr Opin Neurobiol 11:327–335
3. Mayer ML, Westbrook GL, Guthrie PB (1984) Nature 309: 261–263
4. Madison DV, Malenka RC, Nicoll RA (1991) Annu Rev Neurosci 14:379–397
5. Monyer H, Sprengel R, Schoepfer R, Herb A, Higuchi M, Lomeli H, Burnashev N, Sakmann B Seeburg PH (1992) Science 256:1217–1221
6. Kutsuwada T, Kashiwabuchi N, Mori H, Sakimura K, Kushiya E, Araki K, Meguro H, Masaki H, Kumanishi T, Arakawa M (1992) Nature 358:36–41
7. Johnson JW, Ascher P (1987) Nature 325:529–531
8. Kleckner NW, Dingledine R (1988) Science 241:835–837

9a. Laube B, Hirai H, Sturgess M, Betz H, Kuhse J (1997) Neuron 18:493–503

9b. Kemp JA, Bluethmann H, Kew JN (2002) 22:6713–6723

10. Anson LC, Chen PE, Wyllie DJ, Colquhoun D, Schoepfer R (1998) J Neurosci 18:581–589
11. Chatterton JE, Awobuluyi M, Premkumar LS, Takahashi H, Talantova M, Shin Y, Cui J, Tu S, Sevarino KA, Nakanishi N, Tong G, Lipton SA, Zhang D (2002) Nature 415:793-798
12. Matsuda K, Kamiya Y, Matsuda S, Yuzaki M (2002) Brain Res Mol Brain Res 100:43–52

13. Das S, Sasaki YF, Rothe T, Premkumar LS, Takasu M, Crandall JE, Dikkes P, Conner DA, Rayudu PV, Cheung W, Chen HS, Lipton SA, Nakanishi N (1998) Nature 393:377–381
14. Perez-Otano I, Schulteis CT, Contractor A, Lipton SA, Trimmer JS, Sucher NJ, Heinemann SF (2001) J Neurosci 21:1228–1237
15. Ciabarra AM, Sullivan JM, Gahn LG, Pecht G, Heinemann S, Sevarino KA (1995) J Neurosci 15:6498–6508
16. Furukawa H, Gouaux E (2003) EMBO J 22:2873–2885
17. Armstrong N, Gouaux E (2000) Neuron 28:165–181
18. Stern-Bach Y, Bettler B, Hartley M, Sheppard PO, O'Hara PJ, Heinemann SF (1994) Neuron 13:1345–1357
19. Oh BH, Pandit J, Kang CH, Nikaido K, Gokcen S, Ames GF, Kim SH (1993) J Biol Chem 268:11348–1155
20. Lummis SC, Fletcher EJ, Green T (2002) Neuropharmacology 42:437–443
21. Tikhonova IG, Baskin II, Palyulin VA, Zefirov NS (2003) J Med Chem 46:1609–1616
22. Tikhonova IG, Baskin II, Palyulin VA, Zefirov NS, Bachurin SO (2002) J Med Chem 45:3836–3843
23. Kuusinen A, Arvola M, Keinanen K (1995) EMBO J 14:6327–6332
24. Ivanovic A, Reilander H, Laube B, Kuhse J (1998) J Biol Chem 273:19933–19937
25. Keinanen K, Jouppila A, Kuusinen A (1998) Biochem J 330:1461–1467
26. Lichtarge O, Bourne HR, Cohen FE (1996) Proc Natl Acad Sci USA 93:7507–7511
27. Forrest D, Yuzaki M, Soares HD, Ng L, Luk DC, Sheng M, Stewart CL, Morgan JI, Connor JA, Curran T (1994) Neuron 13:325–338
28. Miyamoto Y, Yamada K, Noda Y, Mori H, Mishina M, Nabeshima T (2001) J Neurosci 21:750–757
29. Li Y, Erzurumlu RS, Chen C, Jhaveri S, Tonegawa S (1994) Cell 76:427–437
30. Mohn AR, Gainetdinov RR, Caron MG, Koller BH (1999) Cell 98:427–436
31. Kiefer F, Jahn H, Koester A, Montkowski A, Reinscheid RK, Wiedemann K (2003) Biol Psychiatry 53:345–351
32. Ballard TM, Pauly-Evers M, Higgins GA, Ouagazzal AM, Mutel V, Borroni E, Kemp JA, Bluethmann H, Kew JN (2002) J Neurosci 22:6713–6723
33. Kew JN, Koester A, Moreau JL, Jenck F, Ouagazzal AM, Mutel V, Richards JG, Trube G, Fischer G, Montkowski A, Hundt W, Reinscheid RK, Pauly-Evers M, Kemp JA, Bluethmann H (2000) J Neurosci 20:4037–4049
34. Altschul SF, Madden TL, Schaffer AA, Zhang J, Zhang Z, Miller W, Lipman DJ (1997) Nucleic Acids Res 25:3389–3402
35. Rost B, Sander C (1993) J Mol Biol 232:584–599
36. Thompson JD, Higgins DG, Gibson TJ (1994) Nucleic Acids Res 22:4673–4680
37. Sali A, Blundell TL (1993) J Mol Biol 234:779–815
38. Luthy R, Bowie JU, Eisenberg D (1992) Nature 356:83–85
39. Laskowski RA, MacArthur MW, Moss DS, Thornton JM (1993) Jol Appl Crystal 26:283–291
40. All tools utilized herein were accessed and utilized as implemented in Insight II-97.5, Accelrys (http://www.accelrys.com)
41. Kleywegt GJ, Jones TA (1997) Methods Enzymol 277:525–545
42. Guex N, Peitsch MC (1997) Electrophoresis 18:2714–2723
43. Sayle RA, Milner-White EJ (1995) Trends Biochem Sci 20:374
44. Chothia C, Lesk AM (1986) EMBO J 5:823–826
45. Zvelebil MJ, Barton GJ, Taylor WR, Sternberg MJ (1987) J Mol Biol 195:957–961
46. Baldwin JM (1993) EMBO J 12:1693–1703
47. Zvelebil MJ, Sternberg MJ (1988) Protein Eng 2:127–138
48. Arinaminpathy Y, Biggin PC, Shrivastava IH, Sansom MS (2003) FEBS Lett 553:321–327
49. Arinaminpathy Y, Sansom MS, Biggin PC (2002) Biophys J 82:676–683